Sensory Evolution and Ecology of Early Turtles Revealed by Digital Endocranial Reconstructions

Stephan Lautenschlager [1][†], Gabriel S. Ferreira [2,3,4][†] and Ingmar Werneburg [3,4,5]*

[1] School of Geography, Earth and Environmental Sciences, University of Birmingham, Birmingham, United Kingdom, [2] Biology Department, Faculty of Philosophy, Science, and Letters at Ribeirão Preto, University of São Paulo, Ribeirão Preto, Brazil, [3] Senckenberg Center for Human Evolution and Palaeoenvironment (HEP), Eberhard Karls Universität, Tübingen, Germany, [4] Fachbereich Geowissenschaften der Eberhard Karls Universität, Tübingen, Germany, [5] Museum für Naturkunde, Leibniz-Institut für Evolutions- und Biodiversitätsforschung, Berlin, Germany

In the past few years, new fossil finds and novel methodological approaches have prompted intensive discussions about the phylogenetic affinities of turtles and rekindled the debate on their ecological origin, with very distinct scenarios, such as fossoriality and aquatic habitat occupation, proposed for the earliest stem-turtles. While research has focused largely on the origin of the anapsid skull and unique postcranial anatomy, little is known about the endocranial anatomy of turtles. Here, we provide 3D digital reconstructions and comparative descriptions of the brain, nasal cavity, neurovascular structures and endosseous labyrinth of *Proganochelys quenstedti*, one of the earliest stem-turtles, as well as other turtle taxa. Our results demonstrate that *P. quenstedti* retained a simple tube-like brain morphology with poorly differentiated regions and mediocre hearing and vision, but a well-developed olfactory sense. Endocast shape analysis indicates that an increase in size and regionalization of the brain took place in the course of turtle evolution, achieving an endocast diversity comparable to other amniote groups. Based on the new evidence presented herein, we further conclude that *P. quenstedti* was a highly terrestrial, but most likely not fossorial, taxon.

Keywords: neuroanatomy, sensory adaptation, 3D visualization, digital endocast, stem-turtles, turtle origin

INTRODUCTION

Turtles (Testudinata sensu Joyce et al., 2004) are a diverse group of reptiles with an unusual "bauplan" fundamentally different from that of other amniotes. Unique morphological characters, including the anapsid cranial configuration, which lacks temporal fenestrations, and the presence of a bony shell formed by a dorsal carapace and a ventral plastron have long obfuscated the phylogenetic affinities of turtles (Rieppel, 2007; Lyson et al., 2010). While most molecular studies have recovered turtles nested within diapsid reptiles and often as a sister-group to Archosauria (birds and crocodiles) (Hedges and Poling, 1999; Wang et al., 2013; Field et al., 2014), most studies based on comparative anatomy have placed turtles outside of Diapsida (Gauthier et al., 1988; Lee, 1997; Werneburg and Sánchez-Villagra, 2009; Neenan et al., 2013; Scheyer et al., 2017) or alternatively inside Lepidosauromorpha (deBraga and Rieppel, 1997; Rieppel and Reisz, 1999; Li et al., 2008; Liu et al., 2011). The scant fossil record of stem-turtles (i.e., non-Testudines Testudinata) has further obscured the evolutionary origin of this group. Recent discoveries of new species and reanalysis of existing specimens with novel methodological approaches (e.g., computed

tomography and digital visualization) have provided new data to the debate of turtle ancestry (Li et al., 2008; Bever et al., 2015; Schoch and Sues, 2015). These studies found support for the diapsid origin of turtles and produced potential evidence for closure of the temporal fenestrae early in their evolutionary history (Schoch and Sues, 2015; Werneburg, 2015; Lyson et al., 2016).

Regarding the environmental origin of the group, although all Triassic turtles were clearly terrestrial (Joyce, 2015), data provided by recently described taxa have painted an ambiguous picture regarding the paleoecological setting in which the Testudinata ancestors evolved. While the earliest known potential proto-turtle (i.e., non-Testudinata Pantestudines) *Eunotosaurus africanus* (ca. 260 Ma) has been found in terrestrial environments (Lyson et al., 2016), the somewhat younger *Pappochelys rosinae* (ca. 240 Ma) and *Odontochelys semitestacea* (ca. 220 Ma) were retrieved from lacustrine and deltaic deposits and were considered to have been semi-aquatic (Li et al., 2008; Rieppel, 2013; Schoch and Sues, 2015). In the last two taxa, the dorsoventrally flattened, expanded ribs, and thickened gastralia have been interpreted as adaptations for buoyancy control in an aquatic environment (Schoch and Sues, 2015). In contrast, the morphology of the ribs, as well as the more rigid body wall, powerful forelimbs and triangular skull, have been considered to represent adaptations to fossoriality in *E. africanus* (Lyson et al., 2016). On the other hand, the type localities of both *P. rosinae* and *O. semitestacea* have also yielded terrestrial taxa (Joyce, 2015; Schoch and Sues, 2017) and, in fact, terrestrial diapsid remains are dominant at the type locality of the former (Schoch and Sues, 2015). Additionally, Joyce (2015) argued in favor of *Odontochelys semitestacea* as a terrestrial proto-turtle, based on its phalangeal formula. Hence, terrestrial, fossorial and semi-aquatic habits have all been suggested for the early stages of turtle evolution, before the origin of the protective shell characteristic of the definitely terrestrial stem-turtles (Joyce and Gauthier, 2004; Scheyer and Sander, 2007; Joyce, 2015).

While research on early turtles has focused largely on the acquisition of the anapsid condition and the evolution of the postcranial anatomy employing comparative morphology, histology and genetics, little is known about the endocranial anatomy of stem-turtles (or indeed turtles in general). Using micro-computed tomography (µCT) scanning and digital visualization, we here provide a reconstruction of the endocranial anatomy of *Proganochelys quenstedti*, one of the earliest testudinates from the Late Triassic of Germany. We further compare the reconstructed brain anatomy with different stem- and crown-turtles (Testudines) and other vertebrate taxa using endocast outline analysis to elucidate related anatomical and ecological aspects of turtle origins.

MATERIALS AND METHODS

For digital reconstruction of endocranial anatomy (brain, inner ear, neurovascular structures, nasal cavity) two specimens of *Proganochelys quenstedti* from the Late Triassic of Germany were studied: MB 1910.45.2 (Museum für Naturkunde Berlin) from the Baerecke and Limpricht Quarry, Halberstadt (Jaekel, 1918), and SMNS 16980 (Staatliches Museum für Naturkunde Stuttgart) from the *Plateosaurus*-quarry in Trossingen (Gaffney, 1990). Both specimens consist of nearly complete and articulated cranial skeletons. MB 1910.45.2 shows substantial taphonomic artifacts in the form of anteroposterior shearing and some moderate mediolateral crushing and deformation. However, these artifacts only marginally affect the braincase and the digital reconstruction of the various endocranial structures (see Results for more details).

MB 1910.45.2 was CT scanned at the Leibniz-Institut für Zoo- und Wildtierforschung Berlin/Germany (IZW) using a Toshiba Aquilon ONE medical CT scanner. Scanning parameters were set at 225 kV and 300 µA resulting in an image stack of 512 × 512 × 213 pixels and a voxel size of 2.0 mm per slice. The dataset was subsequently "upsampled" (1024 × 1024 × 426 pixels, 0.5 mm effective voxel size) by averaging the existing slice data. This process does not increase the actual resolution of the data, but provides more slices available for segmentation permitting clearer identification of features and resulting in smoother surface models.

SMNS 16980 was scanned at the Riedberg Campus of Goethe-Universität Frankfurt/Germany using a Phoenix Nanotom m scanner (Werneburg et al., 2015a). Due to its relatively large size, the specimen was scanned in three stages. The resulting image stacks were combined into a single stack with 3583 × 4011 × 5658 pixels and a voxel size of 0.025 mm per slice. The dataset was subsequently downsampled (870 × 954 × 1161 pixels, 0.1 mm voxel size) to permit further processing and segmentation.

Datasets for both specimens were imported into Avizo 8 (Visualization Science Group) for the segmentation of endocranial structures. Due to poor grayscale attenuation (in particular for SMNS 16980), segmentation was performed manually using the paintbrush and interpolation tools in the Avizo segmentation editor (both reconstructions performed by the first author for consistency following Balanoff et al., 2016). 3D surface models and volumes were created to visualize the endocranial components. In addition, surface models of the individual structures were downsampled to a degree that allowed for small file sizes but preserved all details, and were exported as separate OBJ-files for the creation of the interactive 3D-figures provided in the Supplementary Material as outlined in Lautenschlager (2014b) using Adobe 3D reviewer (Adobe Systems Inc.).

To provide a basis for comparisons, the endocranial anatomy of nine extant turtles and of one additional stem-turtle, *Naomichelys speciosa* (FMNH PR273), was reconstructed in the manner described above. FMNH PR273 was scanned at the Institut für Naturwissenschaftliche Archäologie at the Universität Tübingen at a resolution of 0.1 mm resulting in an image stack of 1068 × 1382 × 622 pixels. The following extant species were scanned at the Steinmann-Institut für Geologie, Mineralogie & Paläontologie/Rheinische Friedrich-Wilhelms-Universität Bonn/Germany and at the Museum für Naturkunde Berlin/Germany: *Podocnemis unifilis* (SMF 55470), *Chelodina reimanni* (ZMB Herpetologie 49659), *Emydura subglobosa* (PIMUZ lab# 2009.37), *Pelodiscus sinensis* (IW576-2),

Chelonia mydas (ZMB 37416 MS), *Macrochelys temminckii* (TCGT, Teaching collection Geowissenschaften Towisse), *Emys orbicularis* (WGJ, 1987a), *Platysternon megacephalum* (SMF 69684), *Malacochersus tornieri* (SMF 58702) (see Supplemental Material for Collection abbreviations). Data derived from the reconstructions were further used for a shape analysis of brain morphology.

Due to the absence of unambiguous and consistently identifiable landmarks on the endocast across different amniote taxa, outline shape analysis was performed to quantify morphological differences. Although this approach uses only two-dimensional outlines (in contrast to three-dimensional landmarks), it allows quantification of shape data for geometries lacking homologous landmarks (Haines and Crampton, 2000). For shape analysis, a sagittal cross-section through the surface model of each brain (i.e., digital cast of the endocranial cavity) was produced in Avizo for each reconstruction. Contours of the two-dimensional cross-sections were imported into tpsDig2.16 (Rohlf, 2010), digitized and saved as 1000 x/y-coordinate pairs. All outline data were subsequently analyzed in PAST 3.17 (Hammer et al., 2001) using fast Fourier transformation (FFT) and principal components analysis (PCA) with the hangle module as outlined in Crampton and Haines (1996) and Lautenschlager (2014a). Outlines were smoothed ten times to eliminate pixel noise, and 23 Fourier harmonics were found to describe the outlines of all sampled taxa sufficiently (average Fourier power > 99%) (see also Supplementary Material). In addition to the reconstructed endocasts, further outlines of 52 taxa were collected from the literature (Hopson, 1979; Franzosa, 2004; Neenan and Scheyer, 2012; Bona and Paulina-Carabajal, 2013; Carabajal et al., 2013; George and Holliday, 2013; Herrera et al., 2013; Holloway et al., 2013; Lautenschlager and Butler, 2016; von Baczko and Desojo, 2016; Jirak and Janacek, 2017; Laaß et al., 2017; Paulina-Carabajal et al., 2017; Pierce et al., 2017; Digimorph[1]) for different turtle, archosauromorph, lepidosauromorph and other amniote taxa (for list of taxa see Table S1). These outlines were redrawn in Adobe Illustrator to ensure sufficient resolution for the digitization process. For PCA, each taxon was assigned to a phylogenetic and an ecological (marine, freshwater, terrestrial, fossorial) group. To test for significant differences between those groups, we also conducted a non-parametric MANOVA test (Anderson, 2001) using PC scores representing 95% of total variance transformed into an Euclidean distance matrix, replicated with 10,000 permutations and compared using Bonferroni correction for the *post-hoc* analyses.

RESULTS

Endocranial Anatomy

The reconstruction of MB 1910.45.2 (**Figures 1A–D**) provided most details of the endocranial anatomy, but exhibited some moderate medio-lateral deformation. In comparison, the reconstruction of SMNS 16980 (**Figures 1E–H**) showed no

[1]DigiMorph. *Digital Morphology - A Unique Biological Visualization Library.* Available online at: http://www.digimorph.org/ (Accessed Aug 15, 2017)

obvious artifacts, but the poor grayscale contrast permitted only a few structures (i.e., brain, pituitary fossa and some cranial nerves) to be visualized. In combination, both specimens allowed for a detailed reconstruction of most endocranial components.
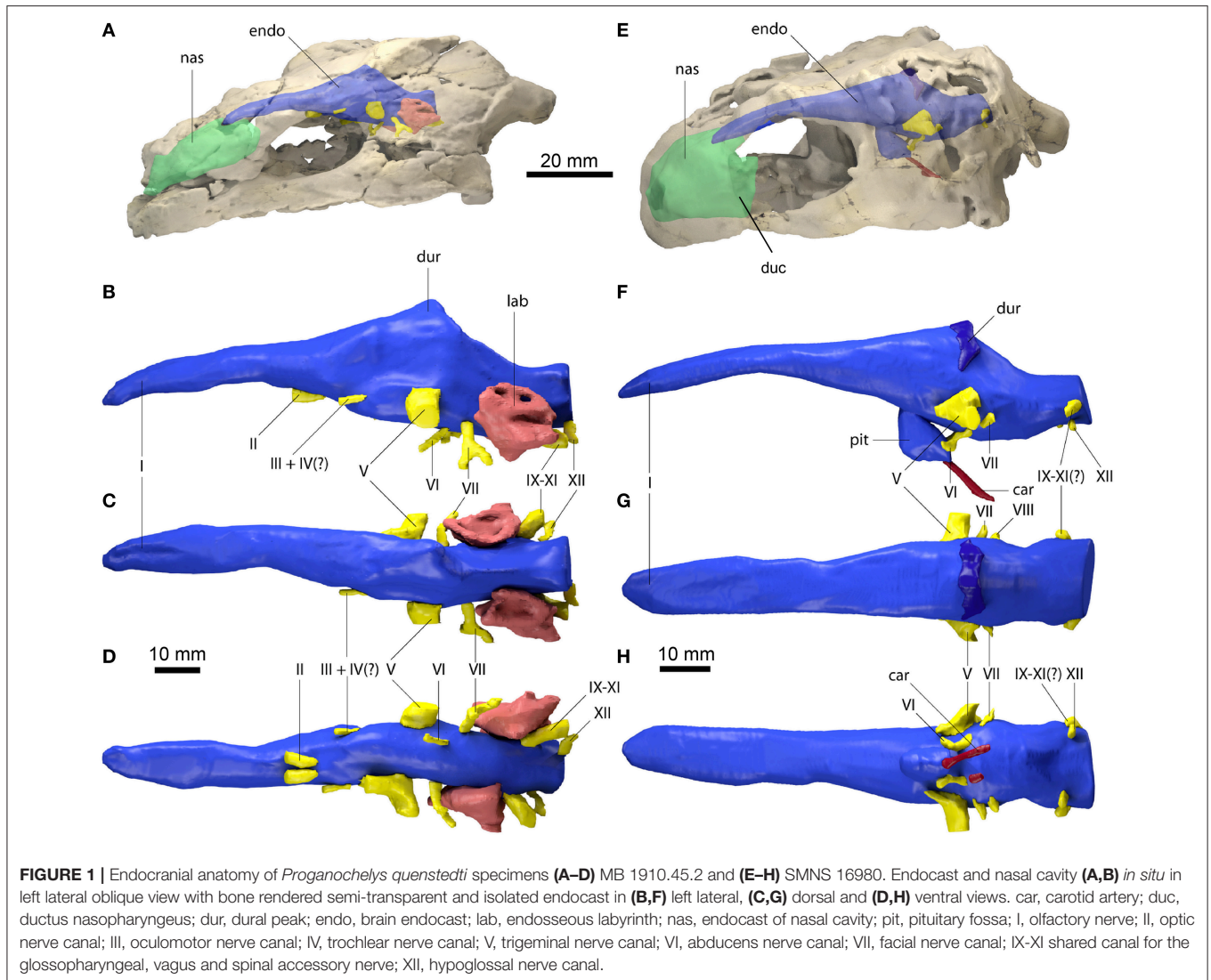
The brain endocast is anteroposteriorly elongate and straight in both specimens, with only moderate cephalic and pontine flexures (**Figures 1B,F**). The endocasts are tubular and mediolaterally narrow without prominent expansion or constriction of the fore-, mid- or hindbrain regions. The close similarity of these features in both specimens confirms that this morphology is natural and unlikely to be a result of taphonomic deformation. The olfactory nerve (CN I) contributes approximately a third to half of the full endocast's length, but a clear distinction between the base of the olfactory nerve and the cerebral hemispheres is not visible. The olfactory bulbs are only weakly reproduced by the ventral surfaces of the nasals. Cerebral hemispheres or distinct optic lobes are not visible in either specimen, suggesting that both structures were very small and/or that the venous sinus and the dura mater obscured the underlying morphology.

The midbrain region is confluent with the forebrain and only weakly demarcated. The only distinguishing feature is a dorsal expansion extending above the level of the olfactory nerve. This dural peak or cartilaginous rider (Zangerl, 1960; Gaffney and Zangerl, 1968; Paulina-Carabajal et al., 2017) is more prominently developed in MB 1910.45.2 (**Figure 1B**). In SMNS 16980, the dorsal expansion is shallower and somewhat separated from the main body of the midbrain by a bony margin, suggesting that this structure corresponds to the cartilaginous portion of the supraoccipital, which ends abruptly anteriorly in *Proganochelys quenstedti* (Gaffney, 1990). The pituitary fossa is visible in SMNS 16980 and forms a pendant pocket, projecting ventrally from the main body of the midbrain endocast.

The hindbrain region is anteroposteriorly short and not constricted mediolaterally between the endosseous labyrinths. Floccular lobes are not visible. Posteriorly, the hindbrain exits the braincase through the foramen magnum, which is oval and wider than high in SMNS 16980 and slightly higher than wide in MB 1910.45.2. The latter may be the result of the mediolateral compression of this specimen.

The nasal cavity is very enlarged when compared to the other sampled taxa (**Figures 2**, **3**; **Table 1**). The strong lateral compression of MB 1910.45.2 may be responsible for the seemingly increased volume, and, hence, we consider the reconstruction of the nasal cavity in SMNS 16980 more reliable. Usually, three portions of the nasal cavity can be identified in turtles and other reptilians (Parsons, 1959, 1970; Halpern, 1992; Paulina-Carabajal et al., 2017): the vestibulum nasi, which connects the nasal chamber to the external nares; the ductus nasopharyngeus, connecting the nasal chamber to the choanae; and the cavum nasi proprium, the chamber itself, bounded anteriorly by the vestibulum, posteroventrally by the ductus, and posterodorsally by the olfactory nerve (CN I). The ductus nasopharyngeus can be distinguished from the rest of the nasal cavity in *P. quenstedti* as two ventrolateral projections (**Figure 1**). A proper duct (at least not bounded by bone) was not expected, since the choanae in *P. quenstedti* are very extensive, and

FIGURE 1 | Endocranial anatomy of *Proganochelys quenstedti* specimens **(A–D)** MB 1910.45.2 and **(E–H)** SMNS 16980. Endocast and nasal cavity **(A,B)** *in situ* in left lateral oblique view with bone rendered semi-transparent and isolated endocast in **(B,F)** left lateral, **(C,G)** dorsal and **(D,H)** ventral views. car, carotid artery; duc, ductus nasopharyngeus; dur, dural peak; endo, brain endocast; lab, endosseous labyrinth; nas, endocast of nasal cavity; pit, pituitary fossa; I, olfactory nerve; II, optic nerve canal; III, oculomotor nerve canal; IV, trochlear nerve canal; V, trigeminal nerve canal; VI, abducens nerve canal; VII, facial nerve canal; IX-XI shared canal for the glossopharyngeal, vagus and spinal accessory nerve; XII, hypoglossal nerve canal.
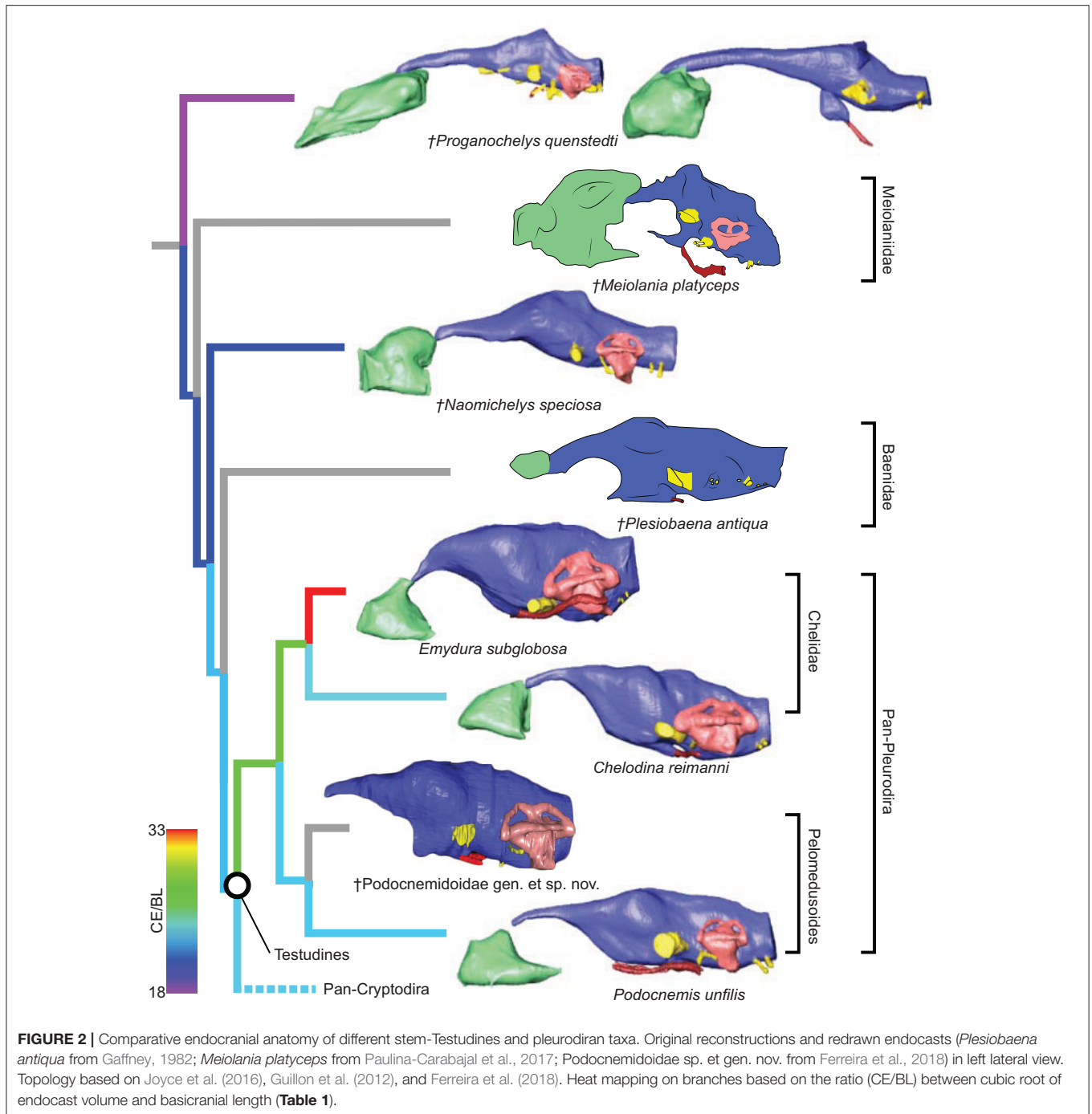
occupy almost the whole ventral surface of the nasal cavity. The vestibulum on the other hand is short, as in most other turtles (Paulina-Carabajal et al., 2017), connected to the large cavum nasi proprium, which constitutes most of the nasal cavity. The cavity as a whole is considerably broad and also high in comparison (**Figures 2**, **3**) to several other taxa (Carabajal et al., 2013; Paulina-Carabajal et al., 2017).

The endosseous labyrinth is reconstructed only for MB 1910.45.2, as the grayscale attenuation did not allow differentiation of the bony housing in SMNS 16980. It is dorsoventrally compressed and compact. The anterior and posterior semicircular canals are small and anteroposteriorly longer than high and have low internal radii. The crus communis is also very low in comparison to other taxa (Carabajal et al., 2013; Mautner et al., 2017; Paulina-Carabajal et al., 2017; Ferreira et al., 2018) which results in an almost horizontal orientation of the anterior and posterior semicircular canals (**Figure 4**). The lateral semicircular canal barely extends laterally from the

vestibulum. The cochlear duct is expanded ventrally, but short. The canal of the fenestra ovalis is clearly visible projecting anterolaterally from the vestibulum.
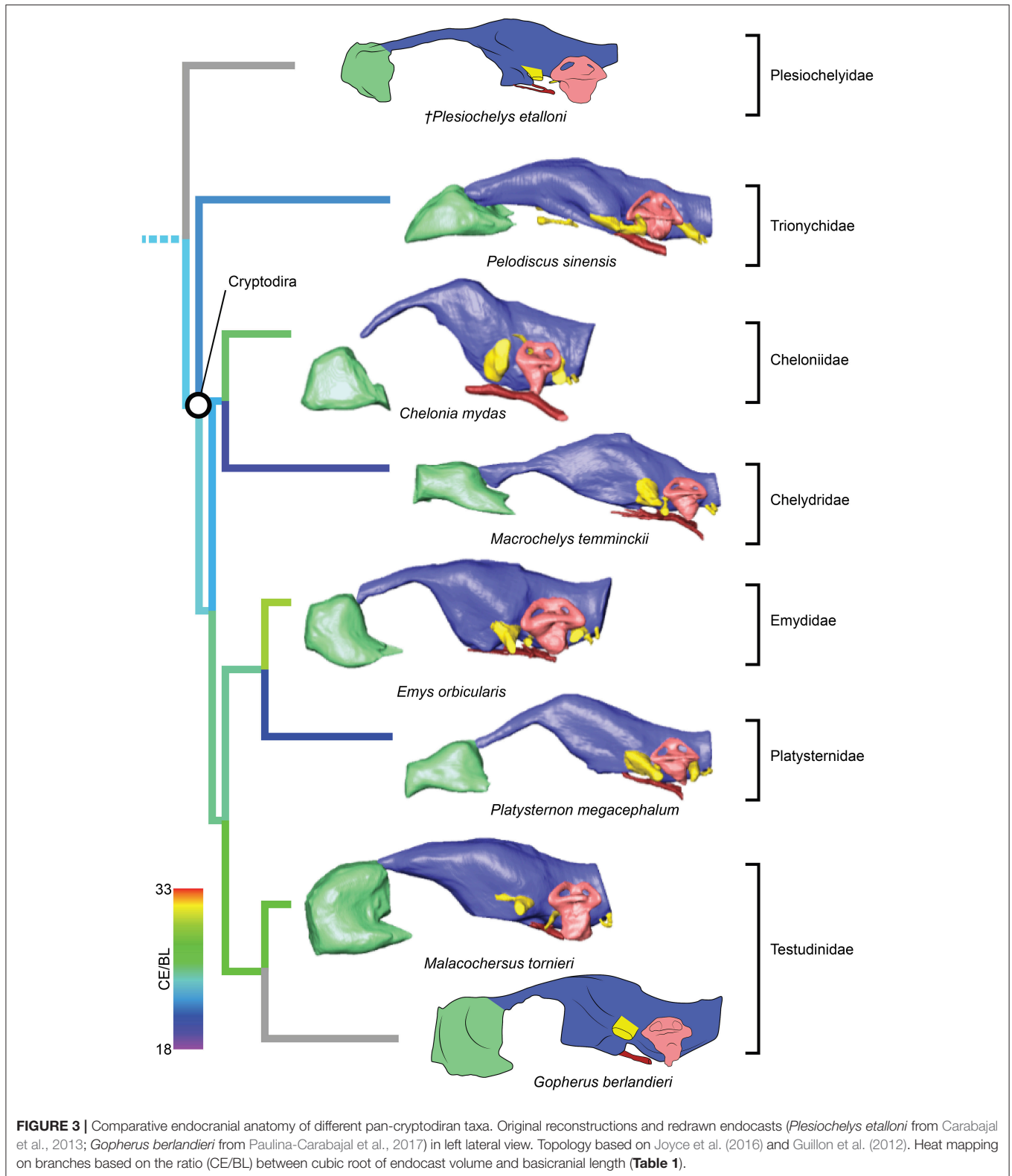
The proximal portion of the majority of cranial nerves could be reconstructed for MB 1910.45.2 (**Figure 1**), whereas only some of the larger nerve canals are visible in SMNS 16980. The optic nerves (CN II) exit the braincase through two large (3 mm in diameter each) foramina anteriorly and ventrally from the cerebral region of the endocast in MB 1910.45.2. Posterior and lateral to CN II, the oculomotor (CN III) and possibly the trochlear nerve (CN IV) (Gaffney, 1990) originate ventrolaterally. In SMNS 16980, CN II-IV could not be reconstructed. The foramina through which those three cranial nerves (II-IV) exit the braincase are formed by the laterosphenoid (="pleurosphenoid") (Gaffney, 1990; Bhullar and Bever, 2009). This is the second *P. quenstedti* specimen with a preserved laterosphenoid, however the fact that this ossification is severely crushed leads us to refrain from commenting

FIGURE 2 | Comparative endocranial anatomy of different stem-Testudines and pleurodiran taxa. Original reconstructions and redrawn endocasts (*Plesiobaena antiqua* from Gaffney, 1982; *Meiolania platyceps* from Paulina-Carabajal et al., 2017; Podocnemidoidae sp. et gen. nov. from Ferreira et al., 2018) in left lateral view. Topology based on Joyce et al. (2016), Guillon et al. (2012), and Ferreira et al. (2018). Heat mapping on branches based on the ratio (CE/BL) between cubic root of endocast volume and basicranial length (**Table 1**).

further on its morphology. The trigeminal nerve (CN V) is large (ca. 6 mm in diameter) and exits the braincase laterally in both specimens through the prootic foramen. Based on both specimens (as well as other specimens described by Gaffney, 1990) we confirm that this foramen is surrounded exclusively by the prootic bone, contrary to Bhullar and Bever's (2009) interpretation that the laterosphenoid would form its anterior margin. A separation of the ophthalmic branch (CN V_1) is apparent on the right side in MB 1910.45.2, but this

could be a result of the high degree of distortion of this specimen.

The abducens nerve (CN VI), clearly visible in both specimens, originates from the ventral surface of the endocast. It pierces the basisphenoid through the foramen nervi abducens and enters laterally the pituitary fossa, which is bottomed by the sella turcica (Gaffney, 1990). Posterior to CN V, the facial nerve (CN VII) exits the braincase laterally through the prootic. In MB 1910.45.2, a distal branching of CN VII outside the braincase

FIGURE 3 | Comparative endocranial anatomy of different pan-cryptodiran taxa. Original reconstructions and redrawn endocasts (*Plesiochelys etalloni* from Carabajal et al., 2013; *Gopherus berlandieri* from Paulina-Carabajal et al., 2017) in left lateral view. Topology based on Joyce et al. (2016) and Guillon et al. (2012). Heat mapping on branches based on the ratio (CE/BL) between cubic root of endocast volume and basicranial length (**Table 1**).

wall is visible, also on the prootic bone. The vestibulocochlear nerves (CN VIII) could not be reconstructed in either specimen. The foramina for the CN VIII branches are usually very small and may lie on cartilaginous structures (Gaffney, 1979), so they are not expected to leave unambiguous traces on fossilized skulls. The glossopharyngeal (CN IX), vagus (CN X) and

TABLE 1 | Measurements and ratios for sampled taxa.

Taxon	Specimen ID	SL [mm]	BL [mm]	EV [mm^3]	NV [mm^3]	N/E	CE/SL	CE/BL	OR [%]	ASC-PSC
Proganochelys	MB 1910.45.2	175	148.75	8,170.84	12,209.34	1.49	11.51	13.54	62.5	107°
Proganochelys	SMNS 16980	97	85.36	3,790.56	3,709.39	0.98	16.07	18.27	57.14	–
Naomichelys	FMNH PR273	117	103.50	9,805.97	4,077.77	0.42	18.29	20.68	15–19	79°
Podocnemis	SMF 55470	67	51.32	1,732.45	531.57	0.31	17.93	23.40	13.39	81°
Chelodina	ZMB H 49659	36	36.00	760.10	140.84	0.18	25.35	25.35	11.34	98°
Chelonia	ZMB 37416 MS	112	80.64	7,077.93	2,667.23	0.38	17.14	23.81	31.65	94°
Macrochelys	GPIT/RE/10801	120	105.88	9,583.53	3,568.33	0.37	17.70	20.06	38.18	88°
Platysternon	SMF 69684	60	46.43	898.13	314.33	0.35	16.08	20.78	28.23	82°
Malacochersus	SMF 58702	35	40.92	1,364.13	669.45	0.49	31.69	27.11	16.06	86°
Emys	WGJ 1987a	31	30.42	668.07	118.54	0.18	28.20	28.74	17.31	102°
Emydura	PIMUZ 2009.37	35	35.00	1,556.29	160.65	0.10	33.11	33.11	9.80	90°
Pelodiscus	IW576-2	59	39.48	707.23	444.09	0.63	15.10	22.57	20.25	79°

ASC-PSC, angle between anterior and posterior semicircular canals; BL, basicranial length; CE/BL, cubic root of endocast volume/basicranial length; CE/SL, cubic root of endocast volume/skull length; EV, endocast volume; NV, nasal cavity volume; N/E, nasal cavity/endocast volume ratio; OR, olfactory ratio; SL, skull length.

accessory nerves (CN XI) originate immediately posterior to the endosseous labyrinth and exit the braincase though the anterior jugular foramen in MB 1910.45.2. Although the sutures are not very clear, this foramen is thought to be formed by the exoccipital, basioccipital and opisthotic in *P. quenstedti* (Gaffney, 1990). In SMNS 16980, a large nerve canal originates in a more dorsolateral position (**Figure 1**). Due to the low resolution, it is unclear whether this canal represents the anterior jugular foramen or parts of the longitudinal sinus, though the latter is more likely. The hypoglossal nerve (CN XII) is transmitted through a single foramen on each side of the basioccipital (posterior to the jugular foramen) in both specimens.

Endocast Outline Analysis

The morphology of the endocast of *Proganochelys quenstedti* was compared to different turtles and other amniote taxa using shape analysis. The PCA results show that the first three PCs account for 71.7% (**Table 2**) of the brain endocast outline shape variation (**Figures 5**, **6**). In no PC plot, there is a clear separation between either the phylogenetic or the ecological groups considered. However, the PERMANOVA tests support that Lepidosauromorpha differs significantly from Archosauromorpha ($p = 0.0006$) and from Testudinata ($p = 0.003$) although these tests find no significant differences between the ecological groups (**Table 3**). The outgroup *Diadectes* is recovered consistently in a position inside the morphospace occupied by other groups, whereas *P. quenstedti* is displaced from the occupied area in all plots; however, on the PC1 axis, *Kawingasaurus* is even more displaced in the positive direction (**Figures 5**, **6**). *P. quenstedti* is distant from other turtles and the minimum spanning-tree (see Supplementary Material) places it closer to the lepidosauromorphs *Placodus* and *Chalarodon*, and to the archosauromorph *Pseudopalatus*, on the PC1/PC2, PC1/PC3, and PC2/PC3 plots, respectively. With regard to the ecological morphospaces, *P. quenstedti* is similarly found in a position outside all the groups, except on the PC1/PC3 plot, on

which it is inside the fossorial morphospace and very close to the terrestrial one (**Figure 6**).

DISCUSSION

Ancestral Condition for Testudinata

Even though more taxa have been assigned to the turtle stem-lineage recently (Li et al., 2008; Lyson et al., 2010; Schoch and Sues, 2015), *Proganochelys quenstedti* remains one of the most important stem-turtles, given its phylogenetic position as the earliest shelled turtle with a completely preserved skull (Parsons, 1959, 1970; Halpern, 1992; Joyce et al., 2016). Its endocast is a relatively simple structure when compared to that of crown-turtles (Carabajal et al., 2013; Mautner et al., 2017; Paulina-Carabajal et al., 2017; Ferreira et al., 2018). It has a tube-like shape, with only small pontine and cephalic flexures and poorly differentiated brain regions. As in other amniotes, the portion between the fore- and midbrain is the most voluminous, but this is achieved exclusively by an increase in height, since the endocast is nearly constant in width over its entire length (**Figure 1**). Another striking feature is the pendant pituitary fossa, which is very common in archosaurs (Witmer et al., 2008; Lautenschlager and Butler, 2016; Araújo et al., 2017; Pierce et al., 2017), but does not occur in extant turtles, in which the dorsum sellae and the sella turcica are aligned, positioning the pituitary fossa approximately at the same level as the posterior portions of the endocast (**Figures 2**, **3**). Although the pituitary fossa of turtles can also house other smaller structures (e.g., internal carotid and abducens nerve) the size of the pituitary gland should be at least partially responsible for the larger size of the fossa in *P. quenstedti*. A similar condition was found for sauropod and theropod dinosaurs (Witmer et al., 2008), in which enlarged pituitary glands have been linked to larger body sizes (Edinger, 1942). While *P. quenstedti* reached a carapace length of at least 67 cm (based on MB 1910.45.2) (Gaffney, 1990), it was not one of the largest turtles, being much smaller than some extant turtles (e.g., up to 150–200 cm in *Chelonia mydas* and
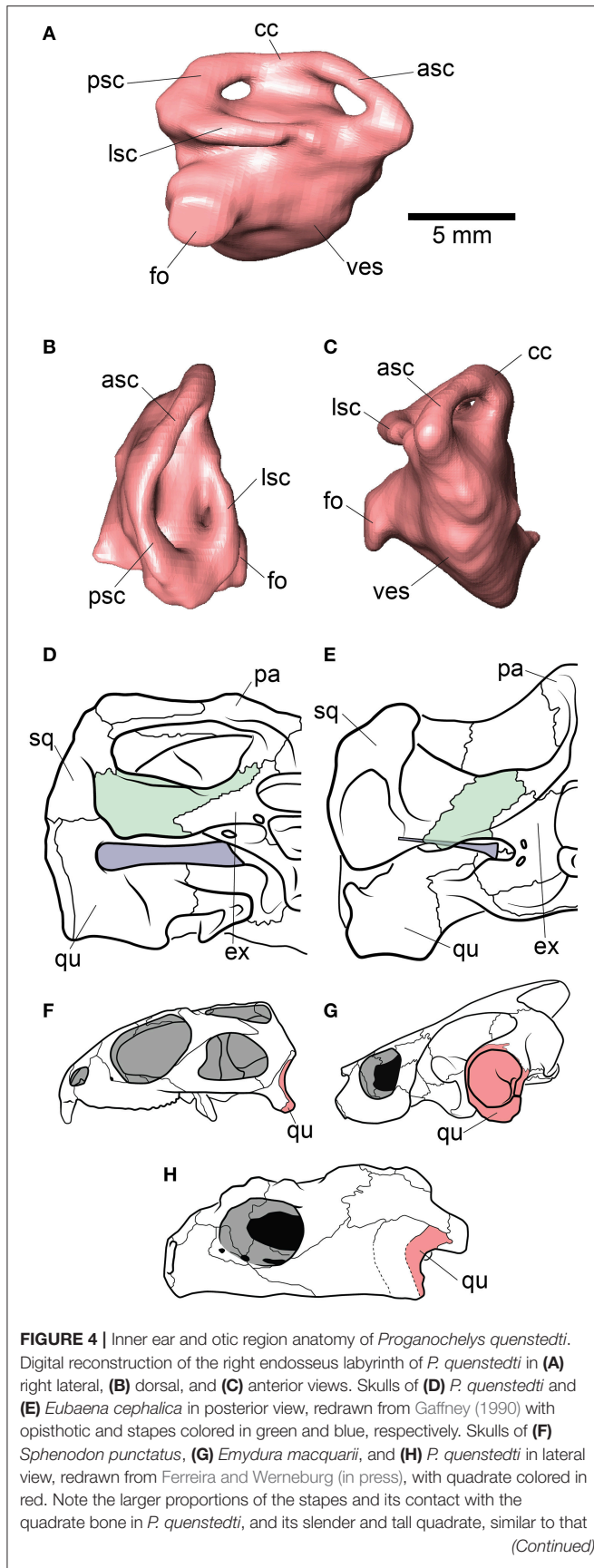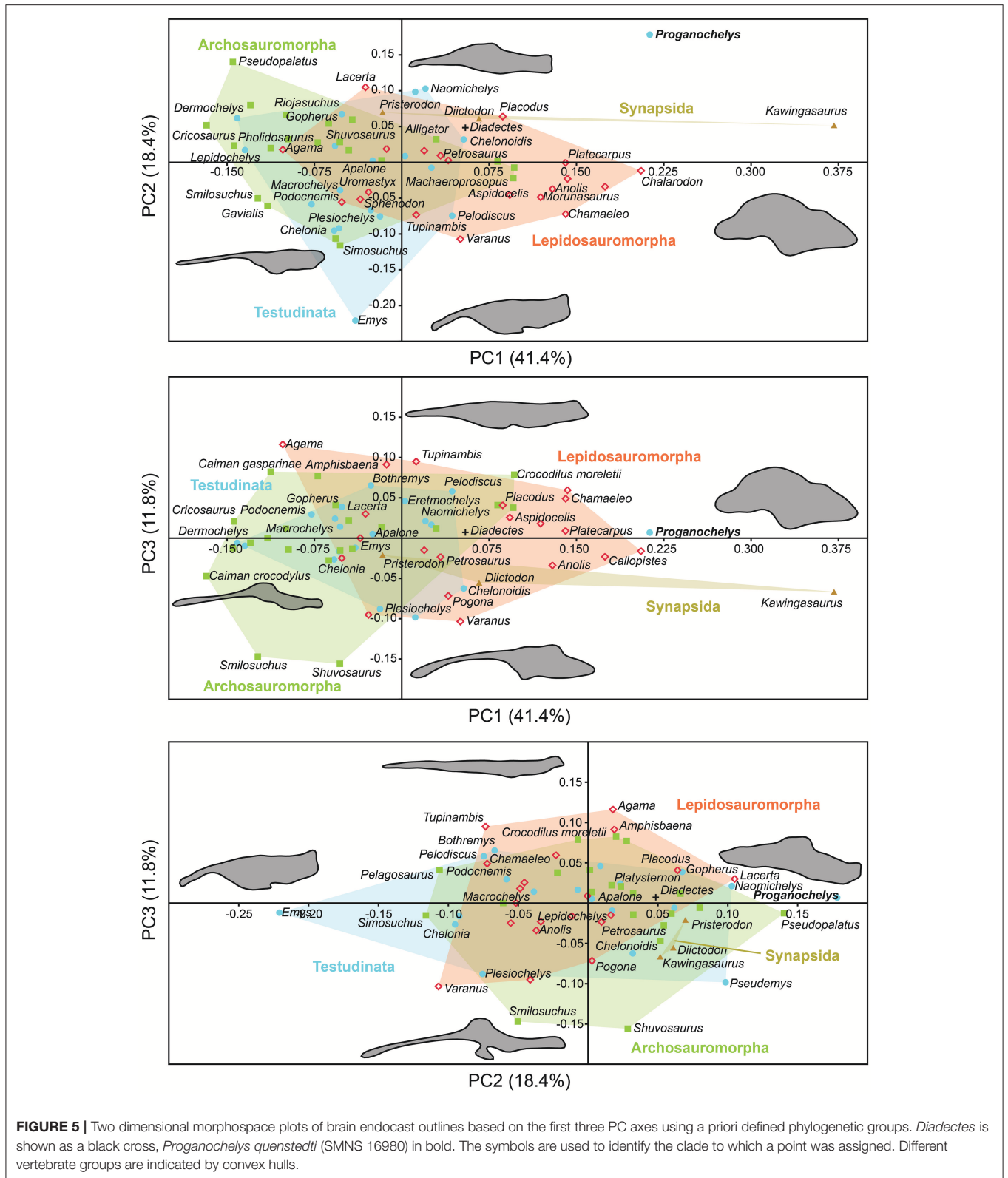
TABLE 2 | Summary of the results of the principal component analyses of the brain outlines of different specimens of turtles and other groups.

PC	Eigenvalue	% variance	% cumulative variance
1	0.01042	41.4	41.4
2	0.00464	18.5	59.9
3	0.00298	11.8	71.7
4	0.00174	6.9	78.7
5	0.00137	5.5	84.1
6	0.00093	3.7	87.8
7	0.00067	2.6	90.5
8	0.00042	1.7	92.1
9	0.00032	1.3	93.4
10	0.00028	1.1	94.5
11	0.00021	0.8	95.4

Pelochelys cantorii) (Angielczyk et al., 2015) and meiolanids (Gaffney, 1996). Turtles included in our sample that are comparable in size to *P. quenstedti*, such as *Podocnemis unifilis* and *Macrochelys temminckii* (up to 68 and 66 cm of carapace length) (Angielczyk et al., 2015), and also *Chelonia mydas*, do not show a pendant pituitary fossa (**Figures 2, 3**). An alternative explanation is that it is not the pituitary fossa that is larger in *P. quenstedti*, but rather the brain that was comparatively smaller. Indeed, in our sample, this taxon has the lowest value for the ratio endocast volume/basicranial length (**Table 1**), supporting the hypothesis that the brain increased in size during turtle evolution.

The brain endocast in turtles does not seem to be consistent with general skull anatomy. Taxa with higher/lower and wider/thinner endocasts do not possess similar skull proportions, which seem more related to the size and shape of the adductor chamber and the associated supraoccipital and squamosal crests (**Figure 7**). Proportional changes observed in the adductor chamber throughout the turtle lineage rather reflect the distinct volume and size of the external jaw adductor musculature in different taxa (Claude et al., 2004; Foth and Joyce, 2016; Foth et al., 2017; Ferreira and Werneburg, in press). Also, the position of the exits of the cranial nerves change only slightly, even with profound changes in the arrangement of related structures such as the eyes and muscles. For example, in *P. quenstedti* the external jaw adductor musculature innervated by the trigeminal nerve (CN V_3) is vertically oriented and entirely positioned anteriorly to the quadrate (Ferreira and Werneburg, in press), while in crown-turtles it extends far posteriorly, following the enlargement of the supraoccipital and squamosal crests (Poglayen-Neuwall, 1953; Werneburg, 2011, 2013). However, the relative position of the exit of CN V remains roughly the same through turtle evolution

FIGURE 4 | Inner ear and otic region anatomy of *Proganochelys quenstedti*. Digital reconstruction of the right endosseus labyrinth of *P. quenstedti* in **(A)** right lateral, **(B)** dorsal, and **(C)** anterior views. Skulls of **(D)** *P. quenstedti* and **(E)** *Eubaena cephalica* in posterior view, redrawn from Gaffney (1990) with opisthotic and stapes colored in green and blue, respectively. Skulls of **(F)** *Sphenodon punctatus*, **(G)** *Emydura macquarii*, and **(H)** *P. quenstedti* in lateral view, redrawn from Ferreira and Werneburg (in press), with quadrate colored in red. Note the larger proportions of the stapes and its contact with the quadrate bone in *P. quenstedti*, and its slender and tall quadrate, similar to that
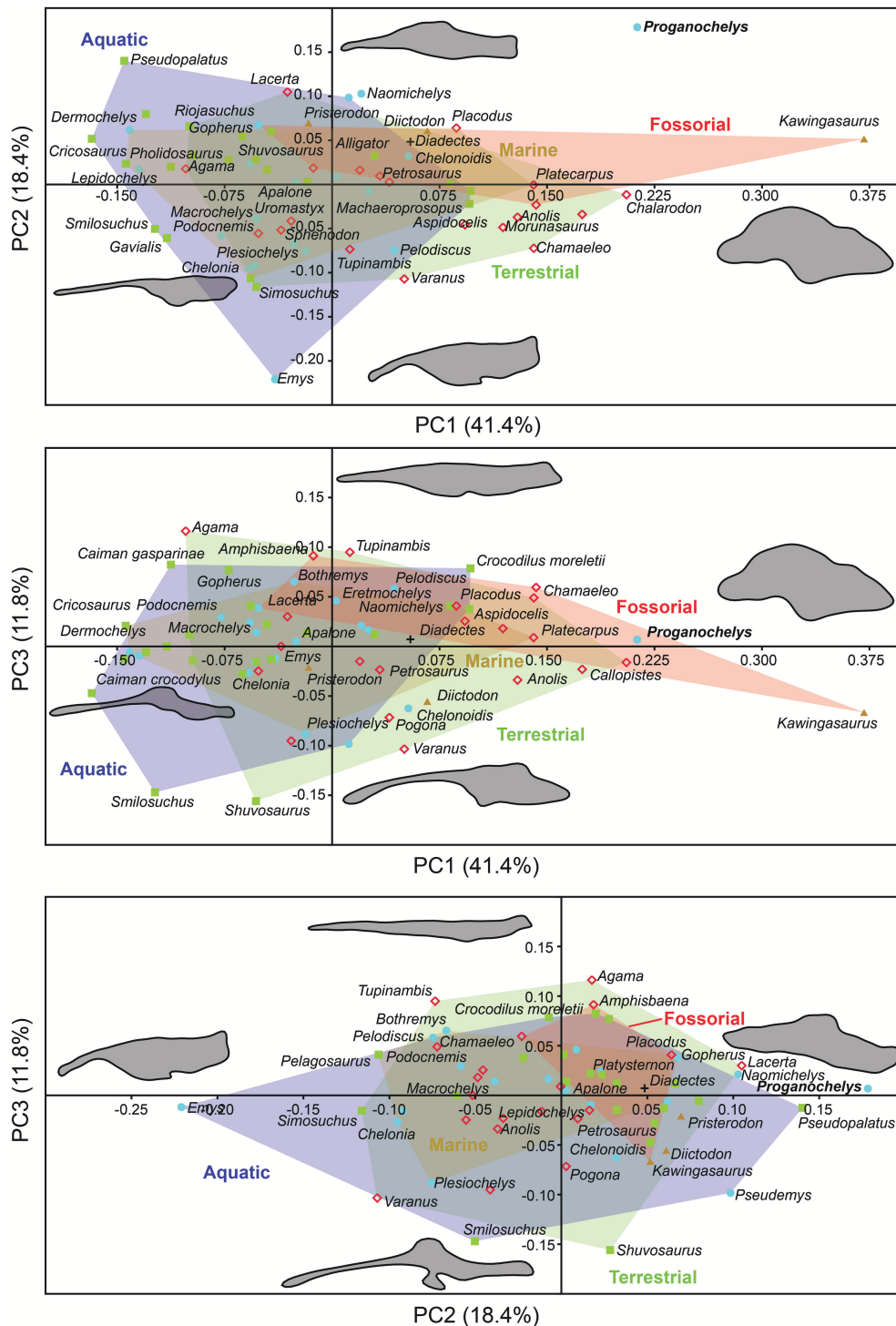
(Continued)

FIGURE 5 | Two dimensional morphospace plots of brain endocast outlines based on the first three PC axes using a priori defined phylogenetic groups. *Diadectes* is shown as a black cross, *Proganochelys quenstedti* (SMNS 16980) in bold. The symbols are used to identify the clade to which a point was assigned. Different vertebrate groups are indicated by convex hulls.

when compared to the remainder of the endocast and the surrounding bones (**Figure 7**). Hence, the actual change that occurs when the muscles expand posteriorly involves only growth and reorientation of distal V_3-branches and not a repositioning of the trigeminal nerve foramen (Poglayen-Neuwall, 1953; Schumacher, 1973).

FIGURE 6 | Two dimensional morphospace plots of brain endocast outlines based on the first three PC axes using a priori defined ecological groups. *Diadectes* is shown as a black cross, *Proganochelys quenstedti* (SMNS 16980) in bold. The symbols are used to identify the clade to which a point was assigned. Different ecological groups are indicated by convex hulls.

Sensory Capabilities of *Proganochelys*

The endosseous labyrinth of *Proganochelys quenstedti* is slightly distinct from that of crown-turtles in being more compact and robust, with short and thick semicircular canals and a low crus communis resulting in almost horizontally oriented canals (**Figure 4**). The anterior and posterior semicircular

TABLE 3 | Results of one-way PERMANOVA test (10000 permutations) with 95% of variance (PC1-PC11), excluding *Proganochelys* and *Diadectes* (for phylogenetic groups only).

PHYLOGENETIC GROUPS			
Permutation N	10000		
Total sum of squares (SQ)	1,901		
Within-group SQ	1,599		
F	3,653		
p	1.00E-01		
	Testudinata	Archosauromorpha	Lepidosauromorpha
Testudinata			
Archosauromorpha	0.8423		
Lepidosauromorpha	0.003	0.0005999	
Synapsida	0.327	0.1056	0.4488
ECOLOGICAL GROUPS			
Permutation N	10000		
Total SQ	77		
Within-group SQ	72		
F	1		
P	0.1656		
	Terrestrial	Aquatic	Marine
Terrestrial			
Aquatic	1		
Marine	0.252	1	
Fossorial	0.6485	1	0.8387

canals (ASC and PSC, respectively) are nearly at the same level as the lateral semicircular canal (LSC), whereas in other turtles the first two run dorsally in relation to the last (Carabajal et al., 2013; Mautner et al., 2017; Paulina-Carabajal et al., 2017; Ferreira et al., 2018). The angle between the ASC and LSC is also very wide (**Table 1**), with similar values to meiolaniids and tortoises (Paulina-Carabajal et al., 2017). This combination of features suggests that the semicircular canals of *P. quenstedti* were not very sensitive during movements within the sagittal (head moving up and down) and coronal planes (head tilt) (Brichta et al., 1988; Spoor et al., 2007; David et al., 2010). Instead, the LSC was likely more effective in stabilizing gaze during yaw movements (head moving left and right). Thus, the labyrinth anatomy of *P. quenstedti* indicates this species was slow and non-agile (Spoor et al., 2007; David et al., 2010), compatible with a highly terrestrial and possibly fossorial lifestyle. This is also tentatively indicated by its position in morphospace outside of, but close to, terrestrial and fossorial groupings in the shape analysis (**Figure 6**).
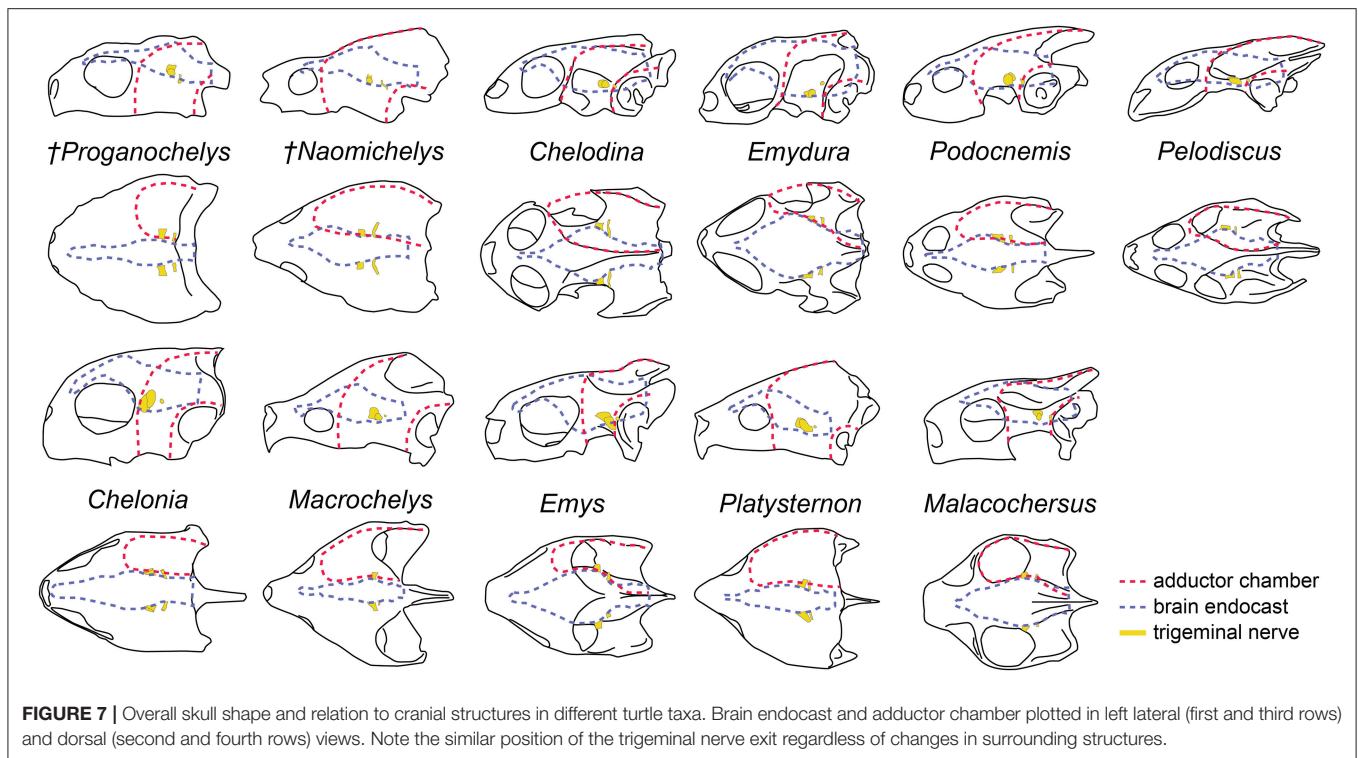
Although the cervical vertebrae of *P. quenstedti* were capable of a certain level of mobility (Werneburg et al., 2015a), its short neck coupled with the relatively low carapace, strong osteoderms on the dorsal neck surface and cervical ribs (Gaffney, 1990) imply restricted mobility along the same planes (sagittal and coronal) (Werneburg et al., 2015a,b) as indicated by its labyrinth morphology. Crown-turtles, however, evolved longer necks and

several taxa are capable of complex and, sometimes, very fast neck and head movements (Poglayen-Neuwall, 1953; Herrel et al., 2008; Werneburg et al., 2015a,b). This could be related to the apparent increase in size of the semicircular canals in crown-turtles (Spoor, 2003; Spoor et al., 2007) when compared to those of *P. quenstedti* (although when compared to more agile reptiles, all turtles possess short canals; Witmer et al., 2008).

Hearing was likely not well-developed in *P. quenstedti*, given the small overall size of the endosseous cochlear duct (Walsh et al., 2009) in comparison to other turtles. Even though its quadrate does not form the characteristic lateral round structure that encloses the cavum tympani in crown-turtles (**Figures 4F–H**), it possibly had a tympanic ear similar to those of extant squamates and cheloniids, in which the tympanum is supported by both bone and connective tissue (Henson, 1974; Gaffney, 1990). However, the stapes of *P. quenstedti* was much stouter than that of crown-turtles (**Figures 4D,E**), and possibly articulated with the quadrate (Gaffney, 1990), suggesting that it was not as effective as the thin vibratory element characteristic of extant amniotes with tympanic hearing, including modern turtles (Baird, 1970; Clack, 1997). As proposed by Clack (1997) for diapsids, elongation of the paraoccipital process of the opisthotic and its tight suturing to the squamosal, which occurred in the group including all testudinates but *Proganochelys quenstedti* (Sterli et al., 2010), may have completely released the stapes from its ancestral structural function (connecting the quadrate to other elements of the braincase) during turtle evolution.

The nasal cavity of *P. quenstedti* represents at least 42.2% of the total endocast volume (**Table 1**), fitting in the volume spectrum of terrestrial turtle taxa, which ranges from 29 to 43% in tortoises and 58.5 to 64% in meiolaniids (Carabajal et al., 2013). Larger nasal cavities have been related to occupation of arid environments, thermoregulation, sound-production or higher olfactory capabilities (Parsons, 1959, 1970; Paulina-Carabajal et al., 2017). In *P. quenstedti*, the cavum nasi proprium represents most of the volume of the nasal cavity and extends far dorsally and posteriorly. Within the nasal cavity, sensory epithelium occurs only on the cavum walls (Parsons, 1970), and, as such, the cavum's relative size could be used as a proxy for inferences about olfactory capability in extinct reptiles. This connection, however, should be interpreted cautiously, due to the possible relation between cavum size and other functions, such as thermoregulation or vocalization (Bourke et al., 2014; Paulina-Carabajal et al., 2017).

The size and volume of the olfactory bulbs have been shown to be related to a greater reliance on the olfactory sense in mammals and birds (Bang, 1971; Bang and Wenzel, 1985; Healy and Guilford, 1990; Gittleman, 1991). In a series of studies the olfactory ratio (ratio between olfactory bulb and cerebral hemisphere maximum diameters; OR values) were used as a proxy to study olfactory acuity and capacity in theropod dinosaurs (including birds) and crocodilians (Zelenitsky et al., 2009, 2011). More recently this has also been applied to turtles (Paulina-Carabajal et al., 2017), showing that tortoises and meiolaniids (both terrestrial taxa) have the highest OR values (36–62 and 20–45%, respectively). Even though OR may not be an exact measure of olfactory acuity it is currently the

FIGURE 7 | Overall skull shape and relation to cranial structures in different turtle taxa. Brain endocast and adductor chamber plotted in left lateral (first and third rows) and dorsal (second and fourth rows) views. Note the similar position of the trigeminal nerve exit regardless of changes in surrounding structures.

best available proxy and its use for a variety of reptilian taxa (Zelenitsky et al., 2009, 2011; Paulina-Carabajal et al., 2017) makes it a useful comparative metric. Here, we show that the OR is even higher in *P. quenstedti*, between 57 and 62% (**Table 1**), but in this case, these values may be also related to the less-developed cerebral hemispheres rather than to larger olfactory bulbs. Nevertheless, the large nasal cavity in association with the high OR values supports our hypothesis that olfaction was possibly the most developed sense in *P. quenstedti*.

Evolution of the Turtle Brain Endocast

In the shape analysis, *Proganochelys quenstedti* is not contained in the morphospace occupied by any of the considered phylogenetic groups (**Figure 5**). There is extensive overlap in the PCA plots, but, at the same time, the PERMANOVA test shows a separation between Lepidosauromorpha, Testudinata and Archosauromorpha (**Table 3**). These results suggest that all amniotes (excluding dinosaurs and mammals) share a similar plesiomorphic brain endocast morphology, but that those lineages evolved in different directions in the morphospace.

Comparing general ecological groups (freshwater, marine, terrestrial, and fossorial) provided similar results, with extensive overlap among the occupied morphospaces (**Figure 6**). *P. quenstedti* is contained in the morphospace occupied by the fossorial group on the PC1/PC3 plot, but it falls outside every group on the other plots. Additionally, the statistical tests do not support significant differences between any of the considered groups (**Table 3**). On the other hand, the minimum spanning trees (see Supplementary Material) show that even when inside the fossorial morphospace *P. quenstedti* is closest to *Placodus*,

a marine lepidosauromorph, and *Pseudopalatus*, an aquatic archosauromorph. A phylogenetic proximity to Sauropterygia (the lepidosauromorph lineage that includes *Placodus*) has been proposed previously (deBraga and Rieppel, 1997) and is associated with the hypothesis that turtles originated in marine environments (Joyce and Gauthier, 2004; Joyce, 2015). The proximity of *P. quenstedti* and *Placodus* in our PC1/PC2 plot (**Figure 6**) may recall this hypothesis, but the poor sampling of sauropterygians together with the extensive overlap between all groups (phylogenetic and ecological) cause us to refrain from considering this a robust interpretation.

The shape analysis presented here is the first attempt to explore the evolution of neuroanatomy in amniotes with a quantitative approach. Even though our results do not support inferences about lifestyles from neuroanatomical data, the significant separation between some of the considered phylogenetic groups (**Figure 5**, **Table 3**) seems promising. We can identify some caveats in our sample (e.g., few marine reptiles, synapsids and early amniotes) that can be easily overcome with the increasing use of computer tomography in paleontological and anatomical studies. Our approach using sagittal cross-section outlines could have also influenced the results, since there is a loss of information when the 3D endocast is simplified to a 2D outline.

More recently, Lyson et al. (2016) thoroughly analyzed the morphology of *Eunotosaurus africanus*, identifying some osteological correlates that led them to conclude that it was likely well-adapted for fossoriality. The authors also identified some of those correlates (e.g., large claws) in other proto- (e.g., *Odontochelys semitestacea*) and stem-turtles (*Proganochelys*

quenstendti and *Palaeochersis talampayensis*), concluding that "fossoriality played an important role in the early evolution of turtles" (Lyson et al., 2016). Although in the PC1/PC3 plot (**Figure 6**) *P. quenstedti* is contained in the fossorial morphospace, the minimum spanning tree (see Supplementary Material) shows it to be closest to the terrestrial non-fossorial taxon *Chalarodon* and the statistical analyses do not support any significant differences between the considered groups (**Table 3**). While the shape analyses do not shed light on this problem conclusively, other sources of data are more convincing. *Proganochelys quenstedti* fossils were found in continental deposits (Gaffney, 1990) and analyses of forelimb proportions (Joyce and Gauthier, 2004) and paleohistology (Scheyer and Sander, 2007) support it as a terrestrial turtle. The morphology of its endosseous labyrinth with short semicircular canals oriented at high angles to each other and the large cavum nasi proprium (Parsons, 1970; David et al., 2010; Paulina-Carabajal et al., 2017) agree with these previous studies, strongly supporting the interpretation that *P. quenstedti* was a well-adapted terrestrial turtle. However, since its vestibule is not particularly large, in contrast to the condition of truly fossorial taxa (Yi and Norell, 2015) or of the semi-fossorial tortoise *Gopherus* (Paulina-Carabajal et al., 2017), the present data suggest it was likely not a fossorial taxon. In *P. quenstedti*, the relatively enlarged vestibule in comparison to the other turtles in this study results from the relatively small semicircular canals. Thus, even if fossoriality had an important role during the early evolution of shell components (Lyson et al., 2016), our data suggests the complete turtle shell first appeared in a terrestrial taxon, with no evident link to fossoriality (at the Testudinata node).

If we assume that the relatively simple morphology of *P. quenstedti* closely resembles that of the testudinate ancestors, some trends can be inferred for the evolution of endocranial structures in turtles. An increase in overall encephalization, for example, with longer and more voluminous endocasts in relation to skull length is found already in the stem-turtle *Naomichelys speciosa* and continues in crown-turtles (**Figures 2**, **3**). Some regions became more pronounced as well. In *N. speciosa*, meiolaniids (Paulina-Carabajal et al., 2017), *Plesiochelys etalloni* (Carabajal et al., 2013) and all other crown-turtles (Mautner et al., 2017; Ferreira et al., 2018) the cerebral hemispheres are clearly distinguishable from the remainder of the endocast and are wider in relation to skull and endocast length than in *P. quenstedti* (**Figures 2**, **3**). The olfactory bulb can also be seen in the endocasts of some taxa, e.g., *Testudo graeca* and *Plesiochelys etalloni* (Carabajal et al., 2013; Paulina-Carabajal et al., 2017). However, this does not seem to be a general trend but rather one of the features that show noteworthy variations among crown-turtles, as are the degree of development of the cephalic and pontine inflections and the sizes of the nasal cavity and the orbits. Considering that the brain of *P. quenstedti* was a simple tube-like structure with poorly differentiated regions, an increase in size and in regionalization of the brain took place later during the course of turtle evolution, similarly (although in a much lesser degree) to the trend observed during bird evolution (Balanoff et al., 2013), and achieved an endocast diversity comparable to other groups of amniotes, such as lepidosaurs and archosaurs (excluding dinosaurs; **Figures 5**, **6**). Indeed, extant turtles possess high brain weights in relation to body weight, comparable to that of crocodiles (Gürtürkün et al., 2016), but that was not the ancestral condition of the group based on our analyses. Given the recurrent results of phylogenetic analyses suggesting that turtles have parareptilian affinity (e.g., Laurin and Piñeiro, 2017), it is important to sample the endocast diversity in that clade and explore the similarities between turtles and all other reptilian lineages. The simpler brain structure together with the large nasal cavity and nearly horizontal and short semicircular canals of the inner ear supports a picture of *P. quenstedti* as a terrestrial but most likely not fossorial turtle, with likely mediocre hearing and vision, but a well-developed olfactory sense.

AUTHOR CONTRIBUTIONS

FUNDING

ACKNOWLEDGMENTS

SUPPLEMENTARY MATERIAL

The Supplementary Material for this article can be found online at: https://www.frontiersin.org/articles/10.3389/fevo.2018.00007/full#supplementary-material

REFERENCES

Anderson, M. J. (2001). A new method for non-parametric multivariate analysis of variance. *Austral Ecol.* 26, 32–46. doi: 10.1111/j.1442-9993.2001.01070.pp.x

Angielczyk, K. D., Burroughs, R. W., and Feldman, C. (2015). Do turtles follow the rules? Latitudinal gradients in species richness, body size, and geographic range area of the world's turtles. *J. Exp. Zool. B Mol. Dev. Evol.* 324, 270–294. doi: 10.1002/jez.b.22602

Araújo, R., Fernandez, V., Polcyn, M. J., Fröbisch, J., and Martins, R. M. (2017). Aspects of gorgonopsian paleobiology and evolution: insights from the basicranium, occiput, osseous labyrinth, vasculature, and neuroanatomy. *Peer. J.* 5:e3119. doi: 10.7717/peerj.3119

Baird, I. L. (1970). "The anatomy of the reptilian ear," in *Biology of the Reptilia*, eds C. Gans and T. S. Parsons (London: Academic Press), 193–275.

Balanoff, A. M., Bever, G. S., Colbert, M. W., Clarke, J. A., Field, D. J., Gignac, P. M., et al. (2016). Best practices for digitally constructing endocranial casts: examples from birds and their dinosaurian relatives. *J. Anat.* 229, 173–190. doi: 10.1111/joa.12378

Balanoff, A. M., Bever, G. S., Rowe, T. B., and Norell, M. A. (2013). Evolutionary origins of the avian brain. *Nature* 501, 93–96. doi: 10.1038/nature12424

Bang, B. G. (1971). Functional anatomy of the olfactory system in 23 orders of birds. *Acta Anat.* 79, 1–76. doi: 10.1159/isbn.978-3-318-01866-0

Bang, B. G., and Wenzel, B. M. (1985). "Nasal cavity and olfactory system," in *Form and function in birds*, eds A.S. King and J. McLelland (New York, NY: Academic Press), 195–225.

Bever, G. S., Lyson, T. R., Field, D. J., and Bhullar, B.-A. S. (2015). Evolutionary origin of the turtle skull. *Nature* 525,239–242. doi: 10.1038/nature14900

Bhullar, B.-A. S., and Bever, G. S. (2009). An archosaur-like laterosphenoid in early turtles (*Reptilia: Pantestudines*). *Breviora* 518, 1–11. doi: 10.3099/0006-9698-518.1.1

Bona, P., and Paulina-Carabajal, A. (2013). Caiman gasparinae sp. nov., a huge alligatorid (Caimaninae) from the late Miocene of Paraná, Argentina. *Alcheringa* 37,1–12. doi: 10.1080/03115518.2013.785335

Bourke, J. M., Ruger Porter, W. M., Ridgely, R. C., Lyson, T. R., Schachner, E. R., Bell, P. R., et al. (2014). Breathing life into dinosaurs: tackling challenges of soft-tissue restoration and nasal airflow in extinct species. *Anat. Rec.* 297, 2148–2186. doi: 10.1002/ar.23046

Brichta, A., Acuña, D., and Peterson, E. (1988). Planar relations of semicircular canals in awake, resting turtles, *Pseudemys scripta*. *Brain Behav. Evolut.* 32,236–245. doi: 10.1159/000116551

Carabajal, A. P., Sterli, J., Müller, J., and Hilger, A. (2013). Neuroanatomy of the marine Jurassic turtle *Plesiochelys etalloni* (Testudinata, Plesiochelyidae). *PLoS ONE* 8:e69264. doi: 10.1371/journal.pone.0069264

Clack, J. (1997). The evolution of tetrapod ears and the fossil record. *Brain Behav. Evolut.* 50, 198–212. doi: 10.1159/000113334

Claude, J., Pritchard, P. C., Tong, H., Paradis, E., and Auffray, J.-C. (2004). Ecological correlates and evolutionary divergence in the skull of turtles: a geometric morphometric assessment. *Syst. Biol.* 53, 933–948. doi: 10.1080/10635150490889498

Crampton, J. S., and Haines, A. J. (1996). *Users' Manual for Programs Hangle, Hmatch and Hcurve for the Fourier Shape Analysis of Two-Dimensional Outlines*, Vol. 96. Science Report, Institute of Geological and Nuclear Sciences.

David, R., Droulez, J., Allain, R., Berthoz, A., Janvier, P., and Bennequin, D. (2010). Motion from the past. A new method to infer vestibular capacities of extinct species. *C. R. Palevol.* 9, 397–410. doi: 10.1016/j.crpv.2010.07.012

Edinger, T. (1942). The pituitary body in giant animals fossil and living: a survey and a suggestion. *Q. Rev. Biol.* 17, 31–45. doi: 10.1086/394644

Ferreira, G. S., Iori, F. V., Hermanson, G., and Langer, M. C. (2018). New turtle remains from the Late Cretaceous of Monte Alto-SP, Brazil, including cranial osteology, neuroanatomy and phylogenetic position of a new taxon. *Paläontol. Zeit*. doi: 10.1007/s12542-017-0397-x

Ferreira, G. S., and Werneburg, I. (in press). "Evolution, diversity, and development of the craniocervical system in turtles with special reference to jaw musculature," in *Heads, Jaws and Muscles – Evolution, Development, Anatomical Diversity and Function,* eds J. Ziermann, R. R. Diaz Jr., and R. Diogo (Heidelberg: Springer).

Field, D. J., Gauthier, J. A., King, B. L., Pisani, D., Lyson, T. R., and Peterson, K. J. (2014). Toward consilience in reptile phylogeny: miRNAs support an archosaur, not lepidosaur, affinity for turtles. *Evol. Dev.* 16, 189–196. doi: 10.1111/ede.12081

Foth, C., and Joyce, W. G. (2016). Slow and steady: the evolution of cranial disparity in fossil and recent turtles. *P. Roy. Soc. Lond. B Bio.* 283m:20161881. doi: 10.1098/rspb.2016.1881

Foth, C., Rabi, M., and Joyce, W. G. (2017). Skull shape variation in extant and extinct Testudinata and its relation to habitat and feeding ecology. *Acta Zool. Stockholm* 98, 310–325. doi: 10.1111/azo.12181

Franzosa, J. W. (2004). *Evolution of the brain in Theropoda (Dinosauria)*. Ph.D. Dissertation, University of Texas, Austin, TX.

Gaffney, E. S. (1979). Comparative cranial morphology of Recent and fossil turtles. *B. Am. Mus. Nat. Hist.* 164, 65–376.

Gaffney, E. S. (1982). Cranial morphology of the baenid turtles. *Am. Mus. Novit.* 2737, 1–22.

Gaffney, E. S. (1990). The comparative osteology of the Triassic turtle *Proganochelys*. *B. Am. Mus. Nat. Hist.* 194, 1–263.

Gaffney, E. S. (1996). The postcranial morphology of *Meiolania platyceps* and a review of of the Meiolaniidae. *B. Am. Mus. Nat. Hist.* 229, 1–166.

Gaffney, E. S., and Zangerl, R. (1968). *A Revision of the Chelonian Genus Bothremys: (Pleurodira: Pelomedusidae)*. Chicago, IL: Field Museum of Natural History.

Gauthier, J. A., Kluge, A. G., and Rowe, T. (1988). "The early evolution of the Amniota," in *The Phylogeny and Classification of the Tetrapods*, Vol. 1, ed M. J. Benton (Oxford: Oxford University Press) 103–155.

George, I. D., and Holliday, C. M. (2013). Trigeminal nerve morphology in *Alligator mississipiensis* and its significance for crocodyliform facial sensation and evolution. *Anat. Rec.* 296, 670–680. doi: 10.1002/ar.22666

Gittleman, J. L. (1991). Carnivore olfactory bulbs: allometry, phylogeny and ecology. *J. Zool.* 225, 253–272. doi: 10.1111/j.1469-7998.1991.tb03815.x

Guillon, J.-M., Guéry, L., Hulin, V., and Girondot, M. (2012). A large phylogeny of turtles (Testudines) using molecular data. *Contrib. Zool.* 81, 147–158.

Gürtürkün, O., Stacho, M., and Ströckens, F. (2016). "The brains of reptiles and birds," in *Evolution of Nervous Systems*, Vol. 1, ed J. H. Kaas (Oxford: Academic Press), 171–221.

Haines, A. J., and Crampton, J. S. (2000). Improvements to the method of Fourier shape analysis as applied in morphometric studies. *Palaeontology* 43, 765–783. doi: 10.1111/1475-4983.00148

Halpern, M. (1992). "Nasal chemical senses in reptiles," in *Biology of the Reptilia*, Vol. 18, eds C. Gans and D. Crews (Chicago, IL; London: University of Chicago Press), 423–523.

Hammer, Ø., Harper, D. A. T., and Ryan, P. D. (2001). Past: paleontological statistics software package for education and data analysis. *Palaeontol. Electr.* 4, 1–9.

Healy, S., and Guilford, T. (1990). Olfactory-bulb size and nocturnality in birds. *Evolution* 44, 339–346. doi: 10.1111/j.1558-5646.1990.tb05203.x

Hedges, S. B., and Poling, L. L. (1999). A molecular phylogeny of reptiles. *Science* 283, 998–1001. doi: 10.1126/science.283.5404.998

Henson Jr, O. (1974). "Comparative anatomy of the middle ear," in *Auditory System*, eds W. D. Keidel and W. D. Neff (Berlin: Springer Verlag), 39–110.

Herrel, A., Van Damme, J., and Aerts, P. (2008). "Cervical anatomy and function in turtles," in *Biology of Turtles*, eds J. Wyneken, M. H. Godfrey, and V. Bels (New York, NY: CRC Press), 163–185.

Herrera, Y., Fernández, M. S., and Gasparini, Z. (2013). The snout of *Cricosaurus araucanensis*: a case study in novel anatomy of the nasal region of metriorhynchids. *Lethaia* 46, 331–340. doi: 10.1111/let.12011

Holloway, W. L., Claeson, K. M., and O'Keefe, F. R. (2013). A virtual phytosaur endocast and its implications for sensory system evolution in archosaurs. *J. Vertebr. Paleontol.* 33, 848–857. doi: 10.1080/02724634.2013.747532

Hopson, J. A. (1979). "Palaeoneurology," in *Biology of the Reptilia,* Vol. 9, ed C. Gans (New York, NY: Academic Press), 39–146.

Jaekel, O. (1918). Die Wirbeltierfunde aus dem Keuper von Halberstadt. Serie II. Testudinata. Teil 1. *Stegochelys* dux, n.g., n.sp. *Paläontol. Zeit.* 2, 88–214. doi: 10.1007/BF03160328

Jirak, D., and Janacek, J. (2017). Volume of the crocodilian brain and endocast during ontogeny. *PLoS ONE* 12:e0178491. doi: 10.1371/journal.pone.0178491

Joyce, W. G. (2015). The origin of turtles: a paleontological perspective. *J. Exp. Zool. B Mol. Dev. Evol.* 324, 181–193. doi: 10.1002/jez.b.22609

Joyce, W. G., and Gauthier, J. A. (2004). Palaeoecology of Triassic stem turtles sheds new light on turtle origins. *P. Roy. Soc. Lond. B. Bio.* 271, 1–5. doi: 10.1098/rspb.2003.2523

Joyce, W. G., Parham, J. F., and Gauthier, J. A. (2004). Developing a protocol for the conversion of rank-based taxon names to phylogenetically defined clade names, as exemplified by turtles. *J. Paleontol.* 78, 989–1013. doi: 10.1666/0022-3360(2004)078<0989:DAPFTC>2.0.CO;2

Joyce, W. G., Rabi, M., Clark, J. M., and Xu, X. (2016). A toothed turtle from the Late Jurassic of China and the global biogeographic history of turtles. *BMC Evol. Biol.* 16:236. doi: 10.1186/s12862-016-0762-5

Laaß, M., Schillinger, B., and Kaestner, A. (2017). What did the "unossified zone" of the non-mammalian therapsid braincase house? *J. Morphol.* 278, 1020–1032. doi: 10.1002/jmor.20583

Laurin, M., and Piñeiro, G. H. (2017). A reassessment of the taxonomic position of mesosaurs, and a surprising phylogeny of early amniotes. *Front. Earth Sci.* 5:88. doi: 10.3389/feart.2017.00088

Lautenschlager, S. (2014a). Morphological and functional diversity in therizinosaur claws and the implications for theropod claw evolution. *P. Roy. Soc. Lond. B Bio.* 281:20140497. doi: 10.1098/rspb.2014.049

Lautenschlager, S. (2014b). Palaeontology in the third dimension: a comprehensive guide for the integration of three-dimensional content in publications. *Paläontol. Zeit.* 88, 111–121. doi: 10.1007/s12542-013-0184-2

Lautenschlager, S., and Butler, R. J. (2016). Neural and endocranial anatomy of Triassic phytosaurian reptiles and convergence with fossil and modern crocodylians. *PeerJ* 4:e2251. doi: 10.7717/peerj.2251

Lee, M. S. (1997). Reptile relationships turn turtle. *Nature* 389, 245–245. doi: 10.1038/38422

Li, C., Wu, X.-C., Rieppel, O., Wang, L.-T., and Zhao, L.-J. (2008). An ancestral turtle from the Late Triassic of southwestern China. *Nature* 456, 497–501. doi: 10.1038/nature07533

Liu, J., Rieppel, O., Jiang, D.-Y., Aitchison, J. C., Motani, R., Zhang, Q.-Y., et al. (2011). A new pachypleurosaur (*Reptilia: Sauropterygia*) from the Lower Middle Triassic of Southwestern China and the phylogenetic relationships of Chinese pachypleurosaurs. *J. Vertebr. Paleontol.* 85, 32–36. doi: 10.1666/09-131.1

Lyson, T. R., Bever, G. S., Bhullar, B.-A. S., Joyce, W. G., and Gauthier, J. A. (2010). Transitional fossils and the origin of turtles. *Biol. Lett.* 6, 830–833. doi: 10.1098/rsbl.2010.0371

Lyson, T. R., Rubidge, B. S., Scheyer, T. M., de Queiroz, K., Schachner, E. R., Smith, R. M. H., et al. (2016). Fossorial origin of the turtle shell. *Curr. Biol.* 26, 1887–1894. doi: 10.1016/j.cub.2016.05.020

Mautner, A. K., Latimer, A. E., Fritz, U., and Scheyer, T. M. (2017). An updated description of the osteology of the pancake tortoise *Malacochersus tornieri* (*Testudines: Testudinidae*) with special focus on intraspecific variation. *J. Morphol.* 278, 321–333. doi: 10.1002/jmor.20640

deBraga, M., and Rieppel, O. (1997). Reptile phylogeny and the interrelationships of turtles. *Zool. J. Linn. Soc. Lond.* 120, 281–354. doi: 10.1111/j.1096-3642.1997.tb01280.x

Neenan, J. M., Klein, N., and Scheyer, T. M. (2013). European origin of placodont marine reptiles and the evolution of crushing dentition in Placodontia. *Nat. Commun.* 4, 1621. doi: 10.1038/ncomms2633

Neenan, J. M., and Scheyer, T. M. (2012). The braincase and inner ear of *Placodus gigas* (*Sauropterygia, Placodontia*)-a new reconstruction based on micro-computed tomographic data. *J. Vertebr. Paleontol.* 32, 1350–1357. doi: 10.1080/02724634.2012.695241

Parsons, T. S. (1959). Nasal anatomy and the phylogeny of reptiles. *Evolution* 13, 175–187 doi: 10.1111/j.1558-5646.1959.tb03003.x

Parsons, T. S. (1970). "The Nose and Jacobson's Organ," in *Biology of the Reptilia*, Vol. 2B, ed C. Gans (New York, NY: Academic Press), 99–191.

Paulina-Carabajal, A., Sterli, J., Georgi, J., Poropat, S. F., and Kear, B. P. (2017). Comparative neuroanatomy of extinct horned turtles (Meiolaniidae) and extant terrestrial turtles (*Testudinidae*), with comments on the palaeobiological implications of selected endocranial features. *Zool. J. Linn. Soc. Lond.* 180, 930–950. doi: 10.1093/zoolinnean/zlw024

Pierce, S. E., Williams, M., and Benson, R. B. (2017). Virtual reconstruction of the endocranial anatomy of the early Jurassic marine crocodylomorph *Pelagosaurus typus* (*Thalattosuchia*). *PeerJ* 5:e3225. doi: 10.7717/peerj.3225

Poglayen-Neuwall, I. (1953). Untersuchungen der Kiefermuskulatur und deren Innervation bei Schildkröten. *Acta Zool. Stockholm* 34, 241–292. doi: 10.1111/j.1463-6395.1953.tb00472.x

Rieppel, O. (2007). "The Relationships of Turtles within Amniotes," in *Biology of Turtles: from Structures to Strategies of Life*, eds J. Wyneken, M. H. Godfrey, and V. Bels (Boca Raton: CRC Press), 345–353.

Rieppel, O. (2013). "The evolution of the turtle shell," in *Morphology and Evolution of Turtles*, eds D. B. Brinkman, P. A. Holroyd, and J. D. Gardner (Heidelberg: Springer), 51–61.

Rieppel, O., and Reisz, R. R. (1999). The origin and early evolution of turtles. *Annu. Rev. Ecol. Syst.* 30, 1–22. doi: 10.1146/annurev.ecolsys.30.1.1

Rohlf, F. (2010). *TPSDig2, Version 2.16.* New York, NY: Stony Brook.

Scheyer, T. M., Neenan, J. M., Bodogan, T., Furrer, H., Obrist, C., and Plamondon, M. (2017). A new, exceptionally preserved juvenile specimen of *Eusaurosphargis dalsassoi* (*Diapsida*) and implications for Mesozoic marine diapsid phylogeny. *Sci. Rep.* 7:4406. doi: 10.1038/s41598-017-04514-x

Scheyer, T. M., and Sander, P. M. (2007). Shell bone histology indicates terrestrial palaeoecology of basal turtles. *P. Roy. Soc. Lond. B Bio.* 274, 1885–1893. doi: 10.1098/rspb.2007.0499

Schoch, R. R., and Sues, H.-D. (2015). A Middle Triassic stem-turtle and the evolution of the turtle body plan. *Nature* 523, 584–587. doi: 10.1038/nature14472

Schoch, R. R., and Sues, H.-D. (2017). Osteology of the Middle Triassic stem-turtle *Pappochelys rosinae* and the early evolution of the turtle skeleton. *J. Syst. Palaeontol.* doi: 10.1080/14772019.2017.1354936. [Epub ahead of print].

Schumacher, G. H. (1973). "The head muscles and hyolaryngeal skeleton of turtles and crocodilians," in *Biology of the Reptilia*, eds C. Gans and T. S. Parsons (London; New York, NY: Academic Press), 101–200.

Spoor, F. (2003). The semicircular canal system and locomotor behaviour, with special reference to hominin evolution. *Courier-Forschungsinstitut Senckenberg* 243, 93–104.

Spoor, F., Garland, T., Krovitz, G., Ryan, T. M., Silcox, M. T., and Walker, A. (2007). The primate semicircular canal system and locomotion. *P. Acad. Nat. Sci. Phila.* 104, 10808–10812. doi: 10.1073/pnas.0704250104

Sterli, J., Müller, J., Anquetin, J., and Hilger, A. (2010). The parabasisphenoid complex in Mesozoic turtles and the evolution of the testudinate basicranium. *Can. J. Earth Sci.* 47, 1337–1346. doi: 10.1139/E10-061

von Baczko, M. B., and Desojo, J. B. (2016). Cranial Anatomy and Palaeoneurology of the Archosaur *Riojasuchus tenuiceps* from the Los Colorados Formation, La Rioja, Argentina. *PLoSOne* 11:e0148575. doi: 10.1371/journal.pone.0148575

Walsh, S. A., Barrett, P. M., Milner, A. C., Manley, G., and Witmer, L. M. (2009). Inner ear anatomy is a proxy for deducing auditory capability and behaviour in reptiles and birds. *Proc. Roy. Soc. Lond. B Bio.* 276, 1355–1360. doi: 10.1098/rspb.2008.1390

Wang, Z., Pascual-Anaya, J., Zadissa, A., Li, W., Niimura, Y., Huang, Z., et al. (2013). The draft genomes of soft-shell turtle and green sea turtle yield insights into the development and evolution of the turtle-specific body plan. *Nat. Genet.* 45, 701–706. doi: 10.1038/ng.2615

Werneburg, I. (2011). The cranial musculature of turtles. *Palaeontol. Electron.* 14, 1–99.

Werneburg, I. (2013). Jaw musculature during the dawn of turtle evolution. *Org. Divers. Evol.* 13, 225–254. doi: 10.1007/s13127-012-0103-5

Werneburg, I. (2015). Neck motion in turtles and its relation to the shape of the temporal skull region. *C. R. Palevol* 14, 527–548. doi: 10.1016/j.crpv.2015.01.007

Werneburg, I., Hinz, J. K., Gumpenberger, M., Volpato, V., Natchev, N., and Joyce, W. G. (2015a). Modeling neck mobility in fossil turtles. *J. Exp. Zool. B Mol. Dev. Evol.* 324, 230–243. doi: 10.1002/jez.b.22557

Werneburg, I., and Sánchez-Villagra, M. R. (2009). Timing of organogenesis support basal position of turtles in the amniote tree of life. *BMC Evol. Biol.* 9:82. doi: 10.1186/1471-2148-9-82

Werneburg, I., Wilson, L. A., Parr, W. C., and Joyce, W. G. (2015b). Evolution of neck vertebral shape and neck retraction at the transition to modern turtles: an integrated geometric morphometric approach. *Syst. Biol.* 64, 187–204. doi: 10.1093/sysbio/syu072

Witmer, L. M., Ridgely, R. C., Dufeau, D. L., and Semones, M. C. (2008). "Using CT to Peer into the Past: 3D Visualization of the Brain and Ear Regions of Birds, Crocodiles, and Nonavian Dinosaurs," in *Anatomical imaging,* eds H. Endo and R. Frey (Tokyo: Springer), 67–87.

Yi, H., and Norell, M. A. (2015). The burrowing origin of modern snakes. *Sci. Adv.* 1:e1500743. doi: 10.1126/sciadv.1500743

Zangerl, R. A. (1960). A new specimen of *Desmatochelys lowii* Williston; a primitive sea turtle from the Cretaceous of South Dakota. *Fieldiana Geol.* 14, 7–40.

Zelenitsky, D. K., Therrien, F., and Kobayashi, Y. (2009). Olfactory acuity in theropods: palaeobiological and evolutionary implications. *Proc. R. Soc. B.* 276, 667–673. doi: 10.1098/rspb.2008.1075

Zelenitsky, D. K., Therrien, F., Ridgely, R. C., McGee, A. R., and Witmer, L. W. (2011). Evolution of olfaction in non-avian theropod dinosaurs and birds. *Proc. R. Soc. B.* 278, 3625–3634. doi: 10.1098/rspb.2011.0238